Neurobiology of Sleep and Circadian Rhythms 13 (2022) 100078

Contents lists available at ScienceDirect

Neurobiology of Sleep and Circadian Rhythms

journal homepage: www.elsevier.com/locate/

Endogenous opioid signaling in the retina modulates sleep/wake activity in mice

Casey-Tyler Berezin [a], Nikolas Bergum [b], Kes A. Luchini [b], Sierra Curdts [c], Christian Korkis [b], Jozsef Vigh [a,b,*]

[a] Cell and Molecular Biology Graduate Program, Colorado State University, 1005 Campus Delivery, Fort Collins, CO, 80523, USA
[b] Department of Biomedical Sciences, Colorado State University, 1601 Campus Delivery, Fort Collins, CO, 80523, USA
[c] Department of Chemical and Biological Engineering, Walter Scott Jr. College of Engineering, Colorado State University, 1376 Campus Delivery, Fort Collins, CO, 80523, USA

ARTICLE INFO

Keywords:
Sleep/wake
Telemetry
μ-Opioid receptor
β-endorphin
Proopiomelanocortin
Retina

ABSTRACT

Circadian sleep/wake rhythms are synchronized to environmental light/dark cycles in a process known as photoentrainment. We have previously shown that activation of β-endorphin-preferring μ-opioid receptors (MORs) inhibits the light-evoked firing of intrinsically photosensitive retinal ganglion cells (ipRGCs), the sole conduits of photoentrainment. Although we have shown that β-endorphin is expressed in the adult mouse retina, the conditions under which β-endorphin is expressed are unknown. Moreover, it is unclear whether endogenous activation of the MORs expressed by ipRGCs modulates the photoentrainment of sleep/wake cycles. To elucidate this, we first measured the mRNA expression of β-endorphin's precursor, proopiomelanocortin (POMC), at various times of day by quantitative reverse-transcription PCR. *POMC* mRNA appears to have cyclic expression in the mouse retina. We then studied β-endorphin expression with immunohistochemistry and found that retinal β-endorphin is more highly expressed in the dark/at night. Finally, we used telemetry to measure activity, EEG and EMG in freely moving animals to compare sleep/wake cycles in wild-type and transgenic mice in which only ipRGCs lack functional MORs. Results from these experiments suggest that the MORs expressed by ipRGCs contribute to the induction and maintenance of activity in the dark phase in nocturnal mice, via the promotion of wakefulness and inhibition of slow-wave sleep. Together, these data suggest that endogenous β-endorphin activates MORs expressed by ipRGCs to modulate sleep/wake activity via the photoentrainment pathway.

1. Introduction

Sleep is an essential behavior across the animal kingdom, but the regulation of sleep states is complex and therefore not fully understood (Scammell et al., 2017; Richter et al., 2014). Across multiple brain regions, there are several neurotransmitter systems and neuropeptides, such as galanin (Richter et al., 2014) and endogenous opioids (Fratta et al., 1987; Myer et al., 1990), that play a role in the central regulation of sleep processes (Scammell et al., 2017; Richter et al., 2014). In addition, sleep is regulated by numerous physiological and environmental factors. Light is the most pervasive environmental factor influencing sleep cycles: circadian sleep/wake rhythms are synchronized to environmental light/dark cycles (i.e. photoentrainment) (LeGates et al., 2014). A classic experiment showed that the photoreceptors driving photoentrainment are in the eye, but they are neither rods nor cones (Freedman et al., 1999), consistent with the fact that non-light perceptive individuals can remain entrained to the 24-h day (Czeisler et al., 1995).

Indeed, a series of studies proved that melanopsin-expressing intrinsically photosensitive retinal ganglion cells (ipRGCs) are the sole conduit of photoentrainment (Berson, 2003; Güler et al., 2008). In addition to transmitting light information to the suprachiasmatic nucleus (SCN) (Fernandez et al., 2016), ipRGCs send monosynaptic projections to sleep-promoting centers, such as the preoptic area (Hattar et al., 2006; Beier et al., 2021), to mediate the acute effects of light on sleep (Altimus et al., 2008; Lupi et al., 2008; Zhang et al., 2021). Neuromodulatory processes inhibiting ipRGCs are expected to alter light-evoked behaviors mediated by ipRGCs, such as photoentrainment and/or pupillary light reflex (PLR) (Güler et al., 2008). Our recent work has shown that ipRGCs express μ-opioid receptors (MORs) and that the

* Corresponding author. Colorado State University, 1617 Campus Delivery, Fort Collins, CO, 80523, USA.
E-mail address: Jozsef.Vigh@colostate.edu (J. Vigh).

https://doi.org/10.1016/j.nbscr.2022.100078
Received 15 April 2022; Received in revised form 16 June 2022; Accepted 20 June 2022
Available online 26 June 2022

MOR-selective agonist [D-Ala^2, MePhe^4, Gly-ol^5]-enkephalin (DAMGO) inhibits light-evoked firing by ipRGCs (Cleymaet et al., 2019). Intraocular injection of DAMGO eliminated PLR triggered by light intensities activating rods and cones, and slowed PLR evoked by bright light sufficient to activate the melanopsin in ipRGCs (Cleymaet et al., 2021). Interestingly, PLR was not inhibited by DAMGO in mice which lacked MORs globally (MKO) or specifically from ipRGCs (McKO), suggesting MORs expressed by ipRGCs are important for mediating the effect of opioids on PLR (Cleymaet et al., 2021). Furthermore, the MOR-selective antagonist D-Phe-Cys-Tyr-D-Trp-Arg-Thr-Pen-Thr-NH_2 (CTAP) enhanced rod/cone-driven PLR in dark-adapted retinas, suggesting that endogenous activation of MORs expressed by ipRGCs in the dark inhibits PLR (Cleymaet et al., 2021).

Opioid receptors in the retina have been shown by numerous studies (Cleymaet et al., 2019; Medzihradsky, 1976; Borbe et al., 1982; Slaughter et al., 1985; Wamsley et al., 1981; Gallagher et al., 2012), and of the endogenous opioid peptides, enkephalins have been detected in amacrine cells of guinea pig (Altschuler et al., 1982) and β-endorphin in a subset of cholinergic amacrine cells of mice (Gallagher et al., 2010). Endogenous opioid peptides are cleaved from larger precursor proteins (Russo, 2017), for example, proopiomelanocortin (POMC) can give rise to β-endorphin as well as non-opioidergic products, such as adrenocorticotropic hormone (ACTH) and α-melanocyte stimulating hormone (α-MSH) (Burbach, 2010; Cawley et al., 2016). However, in the inner retina only β-endorphin, not ACTH nor α-MSH (Gallagher et al., 2010), was detected, consistent with the notion that POMC processing is both cell- and tissue-specific (Bicknell, 2008).

Taken together, there is strong evidence for expression of the endogenous opioid β-endorphin in the adult mammalian retina (Gallagher et al., 2010) and for the activation of β-endorphin-preferring MORs in modulating ipRGC function (Cleymaet et al., 2021). However, it is not known under what conditions retinal β-endorphin is expressed, nor have the neuromodulatory effects of endogenous β-endorphin in the mammalian retina been studied. Accordingly, the aim of the current investigation was two-fold: (1) determine if light exposure and/or circadian timing influences β-endorphin expression in the adult mouse retina, and (2) examine if endogenous β-endorphin signaling in the retina contributes to the photoentrainment of sleep/wake behavior in the nocturnal mouse via MORs expressed by ipRGCs.

2. Materials and methods

2.1. Animals

Wild-type (WT) C57BL/6J mice were purchased from Jackson Laboratories, Bar Harbor, ME (strain #000664). Mice with Cre recombinase expressed upstream of the melanopsin (*Opn4*) promoter [Tg(*Opn4*-cre) SA9Gsat/Mmucd, #036544-UCD; *Opn4*-cre] were purchased from the Mutant Mouse Resource and Research Center (MMRRC) at the University of California at Davis. These *Opn4*-cre mice were backcrossed into a 100% C57BL/6J background prior to purchase and maintained as hemizygotes (*Opn4*-cre +/−). McKO mice, in which only ipRGCs lack functional MORs, were generated as described previously (Cleymaet et al., 2021; Weibel et al., 2013). In brief, *Oprm1*$^{fl/fl}$ breeders (Jackson Labs strain #030074) were generously provided by Dr. Brigitte Kieffer (Douglas Research Center, McGill University). *Oprm1*$^{fl/fl}$ mice have exons 2 and 3 of the MOR (*Oprm1*) gene flanked by a loxP site and were maintained on a 50% C57BL/6J-50% 129Sv background for 5 generations before receipt (Weibel et al., 2013). To establish a 100% C57BL/6J background, *Oprm1*$^{fl/fl}$ mice were backcrossed to WT C57BL/6J mice for ≥10 generations. Finally, *Oprm1*$^{fl/fl}$ and *Opn4*-cre mice were crossed to obtain McKO mice with the floxed *Oprm1* gene on both alleles and *Opn4*-cre on one allele. Mice lacking functional MORs globally (B6.129S2-*Oprm1*^{tm1Kff}/J; MKO) were purchased from Jackson Labs (strain #007559). MKO mice were backcrossed to C57BL/6J mice for at least 12 generations prior to purchase. Adult male and female animals (8–23 weeks) were kept on a 12-h light:12-h dark cycle with lights on at 6:00 a.m. (Zeitgeber time ZT 0), fed standard chow and water ad libitum. Animals were handled in compliance with the Colorado State University Institutional Animal Care and Use Committee and all procedures met the guidelines outlined by the National Research Council's Guide for the Care and Use of Laboratory Animals.

2.2. Reverse transcription quantitative PCR (qRT-PCR)

2.2.1. RNA preparation

Adult male and female mice were anesthetized with Fluriso (isoflurane, VetOne) and euthanized by cervical dislocation or decapitation. Under RNase-free conditions, retinas were microdissected in 0.1 M phosphate buffered saline (PBS; pH 7.4) then placed in RNAlater solution (Sigma-Aldrich) at 4 °C until all samples were collected. Total RNA was extracted using the RNeasy Mini Kit (Qiagen) according to manufacturer's instructions. Briefly, RNAlater solution was washed off by placing the tissue into 0.1 M PBS, then the tissue lysed in Buffer RLT with DTT (GoldBio) by disruption with a micropipette followed by homogenization of the solution by passing it through a 20-gauge needle 5 times. Hypothalami were dissected from the mouse brain and immediately homogenized in Buffer RLT with DTT (GoldBio) by passing it through 20-gauge and 27-gauge needles 5 times each. The lysate was centrifuged, and the supernatant combined with 70% ethanol before being put on the column. After RNA was eluted from the column, the concentration and quality (A_{260}/A_{280}) of each sample was assessed using a Nanodrop (ThermoFisher NanoDrop2000 or ThermoFisher NanoDrop Lite). Genomic DNA (gDNA) was digested using DNase I, RNase-free (ThermoFisher) according to manufacturer's instructions. RNA concentration was again measured using a Nanodrop, and RNA integrity and successful DNase treatment was assessed on a 1% agarose gel. All samples displayed strong 28S and 18S rRNA bands, no gDNA contamination, and no degradation.

2.2.2. Reverse transcription

Reverse transcription of RNA was performed using the GoScript™ Reverse Transcription System (ProMega) according to manufacturer's instructions. 200 ng RNA was used in each reaction and a no-reverse transcription (NRT) control was performed alongside each sample. cDNA was stored at −20 °C until used for qRT-PCR amplification.

2.2.3. qRT-PCR primer design

Primers and probes were designed using Integrated DNA Technologies' PrimerQuest™ Tool. For each target, primers were designed to span an exon-exon junction, have melting temperatures between 60 °C and 65 °C, have GC content between 45 and 65%, and be no more than 30 nucleotides long. Probes were designed to have melting temperatures at least 5 °C higher than the primers, have GC content between 45 and 75%, and be no more than 30 nucleotides. Amplicons were required to be shorter than 150 nucleotides. All other parameters were left to the default. The multiplexed primers (500 nM) and probe (250 nM) were resuspended in IDTE buffer (10 mM Tris, 0.1 mM EDTA in H_2O) upon receipt then stored at −20 °C.

For each primer set, a temperature gradient was used to determine the optimal annealing temperature. Reaction parameters were first determined in singleplex reactions before multiplexing. PCR products from each primer set were run on a 2% agarose gel to assess the specificity of the primers. For all genes, one clear band was seen with no gDNA contamination or additional products.

In the mouse retina, *β-actin* is a commonly used reference gene (Sawant et al., 2017) and *Tbp* has been shown to be an appropriate reference gene (Adachi et al., 2015). Both genes were stably expressed in all samples. For the *Oprm1* (MOR) experiments, both *Tbp* and *β-actin* were used as reference genes. For the *POMC* experiments, only *Tbp* was used as a reference gene because the cycling requirements for *β-actin* were not compatible with the requirements for *POMC*. Primer and probe

sequences can be found in Table 1.

2.2.4. qRT-PCR protocol

Reactions were set up using GoTaq® Probe qPCR Master Mix (ProMega) according to manufacturer's instructions, however because our primers and probes arrived multiplexed, only 1 μL was used and an additional 2 μL of nuclease-free water was added in the total 20 μL reaction mix.

The cycling conditions for *POMC* were as follows: 2 min, 95 °C, GoTaq® DNA polymerase activation, then 35 cycles of denaturation (95 °C, 15 s) and annealing/extension (63.2 °C, 30 s). The cycling conditions for *Oprm1* were as follows: 2 min, 95 °C, GoTaq® DNA polymerase activation, then 35 cycles of denaturation (95 °C, 15 s) and annealing/extension (57.2 °C, 30 s).

Each plate contained a standard curve, run in triplicate, which included three 10-fold dilutions. Every experimental sample was run in triplicate using 2 μL of cDNA. A NRT control and no-template control (H_2O instead of cDNA or RNA; NTC) was included in each run. No amplification was seen in any NRT or NTC controls. Assay plates were prepared in-lab then run on a CFX96 Touch Real-Time PCR Detection System (BioRad).

2.2.5. Data analysis

The CFX Manager™ Software, version 3.1 (BioRad) was used to set the threshold for each reaction (highest R^2 just above the background) and to assess the efficiency of the reaction based on the standard curve (90–110%). It was also used to normalize data between plates when samples needed to be re-run or run on multiple plates. In these cases, at least one identical sample was run on each plate and used as an inter-run calibrator. The quantification cycle (Cq) values for each experiment were downloaded as an Excel spreadsheet and the ΔΔCt method was used for analysis (Livak and Schmittgen, 2001; Hellemans et al., 2007). For each gene, the Cq values for all samples in the control group were averaged and used as the reference to calculate relative gene expression (RGE) in each sample. Where multiple reference genes were used, the geometric mean of those genes' relative quantities was used to calculate RGE (Vandesompele et al., 2002).

2.3. Immunohistochemistry

Both adult male and female mice were adapted to the light condition (i.e. light or dark) for at least 2 h before anesthetization with Fluriso (isoflurane, VetOne) and sacrificed by cervical dislocation. For daytime β-endorphin measurements, mice were sacrificed between ZT 4 and ZT 8. For nighttime β-endorphin measurements, mice were sacrificed between ZT 19 and ZT 20, as indicated by previously reported β-endorphin peak levels in the brain (Kerdelhue et al., 1983; Jamali and Tramu, 1999; Labrecque and Vanier, 1995). In dark-adapted conditions, mice were sacrificed and retinas microdissected under infrared illumination with the aid of OWL Night Vision Scopes (BE Meyers) mounted on Olympus SZ51 stereoscopes to maintain the retina in a fully dark-adapted state. Mice were enucleated and the eyes placed in 0.1 M PBS, then a small incision was made at the ora serrata and the whole eye fixed in freshly prepared 4% paraformaldehyde (PFA) in PBS for 20 min at room temperature (RT). Retinas were then dissected out in PBS and placed in the same fixative solution for an additional 5 min. Retinas were washed 3 × 20 min in 0.1 M PBS at RT, then incubated in a blocking solution (5% serum and 0.5% Triton X-100 in PBS) for 3 h on a shaker table at RT. Retinas were incubated in primary antibodies diluted in the blocking solution for at least 30 h on a shaker table at RT (goat anti-choline acetyltransferase 1:200, Millipore; rabbit anti-β-endorphin 1:5000, NHPP-NIDDK). Retinas were then washed (3 × 20 min) in PBS and incubated, either at RT for 4 h or overnight at 4 °C, in the appropriate secondary antibodies. After a final 3 × 20 min wash in PBS, retinas were mounted on Superfrost Plus microscope slides (Fisher Scientific) in Vectashield Plus Antifade Mounting Medium (Vector Laboratories, Burlingame, CA).

2.4. RNAscope in situ hybridization

Adult male and female mice were anesthetized with Fluriso (isoflurane, VetOne) and euthanized by cervical dislocation. Under RNase-free conditions, eyecups were dissected in 0.1 M PBS, fixed in cold 4% PFA for 25 min, and immersed in 30% sucrose at 4 °C for several days prior to being embedded in Optimal Cutting Temperature (O.C.T.) Compound (Tissue-Tek). The tissue was sectioned at 20 μm on a ThermoFisher CryoStar NX50 cryostat, directly applied to SuperFrost Plus slides (Fisher Scientific), and stored at −20 °C until use. The RNAscope Multiplex Fluorescent Assay v2 was performed according to the manufacturer's protocol for fixed-frozen tissue (Advanced Cell Diagnostics, Newark, CA). In brief, after washing off the OCT with PBS, slides were baked at 60 °C in the HybEZ Oven (ACDbio) for 30 min. Slides were post-fixed in 4% PFA for 15 min, then dehydrated in a series of ethanol gradients at room temperature for 5 min each (50%, 70%, 100% x2). During pretreatment, slides were boiled in the supplied Target Retrieval reagents for 15 min. The probes used were specific to sequences in the *Oprm1* (*Mus musculus* opioid receptor mu 1 #544731) and *Opn4* (*Mus musculus* opsin 4 [melanopsin] #438061-C2) genes. Probes were labeled with Opal dyes 520 and 570 (Akoya Biosciences), respectively. Opal dyes were used at a 1:1500 dilution initially then adjusted according to signal intensity (i.e. increased to 1:1000 for *Oprm1*).

2.5. Confocal laser microscopy

All images were obtained on a Zeiss LSM 900 confocal microscope (Carl Zeiss, Oberkochen, Germany). For all acquisitions, sequential scans at the different wavelengths were performed. For immunohistochemical experiments performed in whole-mount retinas, tiling was used to capture 1 mm^2 images including the center and periphery regions of the retina. Where high-quality images of this size could not be taken in the remaining periphery regions, additional images were at least 300 μm^2. All images were taken at 0.5 or 1 μm increments through

Table 1
Primer and probe sequences for qRT-PCR experiments.

Target	Forward Primer (5′-3′)	Reverse Primer (5′-3′)	Probe Sequence (5′-3′)	Notes
Proopiomelanocortin (*Pomc*), NM_001278581.1, transcript variant 1	GATGCAAGCCAGCAGGT	GATTCTGCTACAGTCGCTCAG	/6-FAM/ATAGATGTG/ZEN/ TGGAGCTGGTGCCTG/IABkFQ/	This is the longest transcript of 5 transcripts that produce the same protein and only differ in their 5′ UTR.
Opioid receptor, mu 1 (*Oprm1*), NM_001304955.1, transcript variant MOR-1U	ACGTGAGGGTGCAATCTATG	GCAACTGGATCCTCTCTTCTG	/6-FAM/CTGCCCGTA/ZEN/ ATGTTCATGGCAACC/IABkFQ/	This is the longest transcript.
β-actin (*Actb*), NM_007393.5	GTCATCCATGGCGAACTGG	ACTGTCGAGTCGCGTCC	/HEX/CGTTGCCGG/ZEN/ TCCACACCCGCCA/IABkFQ/	This is the only transcript.
TATA box binding protein (*Tbp*), NM_013684.3	CCATGAAATAGTGATGCTGGGC	GGGTATCTGCTGGCGGTTT	/HEX/TGCGGTCGC/ZEN/ GTCATTTTCTCCGCAGT/ IABkFQ/	This is the only transcript.

the ganglion cell layer (GCL) and inner nuclear layer (INL) with a 20× air objective. Somas immunopositive for ChAT and β-endorphin in the same optical section were counted manually and totaled using the Cell Counter plugin (De Vos, University of Sheffield) in Fiji (Schindelin et al., 2012). For RNAscope in situ hybridization experiments, Z-stack images were taken at 0.5–1 μm increments through the full thickness of the sections with a 40× oil-immersion objective. Quantitative analysis was performed on projections of all Z-stacks using Fiji (Schindelin et al., 2012).

2.6. Surgery & telemetry recordings

Adult male WT and McKO mice were surgically implanted with mini-telemetry transmitters (HD-X02, DSI) as previously described (Zhang et al., 2021; Locklear, 2020). In brief, mice were deeply anesthetized with isoflurane (5%) and fitted with a nose cone for continuous isoflurane delivery (1–5%). Core body temperature and respiratory rate were monitored throughout surgery. Transmitters were subcutaneously inserted in the dorsal abdomen, electromyogram (EMG) leads were inserted into the cheek muscles, and electroencephalogram (EEG) leads were placed into holes drilled into the skull (1.0 mm posterior to bregma, 1.0 mm left of midline; 2.0 mm posterior to bregma, 1.0 mm right of midline). A screw was drilled into the skull (2.5 mm posterior to bregma, 1.0 mm left of midline), and dental acrylic was used to adhere the leads to the skull and the screw. After the incisions were sutured, mice received an injection of the non-steroidal anti-inflammatory drug (NSAID) OstiLox (3 mg/kg meloxicam, VetOne) and their status was recorded every 5 min for the first 30 min post-surgery. Mice continued to be monitored for 3 days in separate cages under a standard 12-h light:12-h dark cycle with lights on at 7:00 a.m. (ZT 0). After recovery, each cage was placed on a receiver (DSI), which relayed the telemetry signals to a computer for recording.

2.6.1. Activity measurements

The implanted transmitters recorded the x-y movement of WT and McKO mice in their cages for at least 4 days continuously. Activity, measured in arbitrary units, was recorded each minute. Mice were considered inactive when no x-y movement was recorded during that minute. Data analysis was performed using the *Rethomics* set of R packages, a framework for high-throughput behavioral analysis (Geissmann et al., 2019).

2.6.2. Sleep/wake measurements

The implanted transmitters recorded activity, EEG and EMG data from WT and McKO mice for at least 3 days continuously. Artifacts in recording were minimized in Neuroscore software (DSI) using Nan Substitution of the previously recorded value. Wake, slow-wave sleep (SWS), or paradoxical (REM) sleep were scored automatically by the software in 10-s epochs. In brief, wake is characterized by low-amplitude EEG and high-amplitude EMG/activity, SWS by high-amplitude EEG and low-amplitude EMG/activity, and REM sleep by low-amplitude EEG and low-amplitude EMG/activity (McDowell et al., 2014; Borniger et al., 2013).

2.7. Statistical analysis

Statistical tests were performed in either R (version 4.1.2) or SigmaPlot (version 11.2). For all tests, $p < 0.05$ was considered significant. The qRT-PCR data was analyzed by *t*-test (McKO validation in retina) or ANOVA (POMC measurements, McKO validation in retina/hypothalamus), immunohistochemical data analyzed by multivariate ANOVA, and RNAscope data analyzed by *t*-test. The behavioral data were analyzed by ANOVA in most cases, except for the whole-day sleep/wake recordings which were analyzed by the non-parametric Wilcoxon rank-sum test due to non-normality and non-homogenous variance of the data. ANOVAs were followed by Tukey-adjusted post-hoc pairwise comparisons. Where multiple measurements were made from the same mouse (e.g. qRT-PCR in the retina and hypothalamus; behavioral experiments) a linear mixed effects model was fit to the data.

3. Results

3.1. POMC mRNA expression in the retina appears to have cyclic variation across the day

Some evidence suggests that *POMC* mRNA is more highly expressed at night in the rodent hypothalamus, particularly in the arcuate nucleus (Orozco-Solís et al., 2011; Agapito et al., 2014; Chen et al., 2004; Steiner et al., 1994). POMC expression is known to be region- and tissue-specific (Bicknell, 2008), and to our knowledge, no studies have assessed changes in *POMC* mRNA throughout the day in the mammalian retina. Thus, we used quantitative reverse-transcription PCR (qRT-PCR) to quantify *POMC* mRNA in the retina and hypothalamus of male WT mice sacrificed at the midpoint of the light phase [Zeitgeber time (ZT) 6, n = 5] or the dark phase (ZT 18, n = 5). At ZT 18, mice were sacrificed and the retinas dissected under infrared illumination to maintain the animals in a dark-adapted state. The expression of *POMC* in each sample, relative to the reference gene *Tbp*, was calculated using the retina samples at ZT 6 as the control group. Relative gene expression values were log-transformed in order to satisfy the assumptions of ANOVA. We found that there was a significant interaction of light condition and tissue type ($F_{1,8} = 11.17$, $p = 0.0102$, ANOVA). In the retina, there was significantly less *POMC* mRNA at ZT 6 compared to ZT 18 ($t(15.7) = -3.025$, $p = 0.0082$; Fig. 1a). At ZT 6, *POMC* expression in the hypothalamus was about 60-fold higher than in the retina (4-fold on the log scale, $t(8) = 18.609$, $p < 0.0001$; Fig. 1b, Supp. Fig. 1a). At ZT 18, *POMC* expression in the hypothalamus was about 40-fold higher than in the retina (3-fold on the log scale, $t(8) = 13.883$, $p < 0.0001$; Fig. 1b, Supp. Fig. 1b). Interestingly, we did not find that *POMC* mRNA in the hypothalamus was different between ZT 6 and 18 ($t(15.7) = 1.362$, $p = 0.1924$; Fig. 1b).

We wanted to elicit further information on potential cyclic variations in *POMC* mRNA expression in the mouse retina, so we sacrificed male WT mice every 8 h [ZT 2 (n = 6), ZT 10 (n = 6), and ZT 18 (n = 5)] (Fig. 1c). Sample collections at ZT 18 were again performed under infrared illumination in accordance with the light-dark cycle. In this experiment, we found that the time-of-day was not a significant predictor of retinal *POMC* mRNA expression ($F_{2,14} = 0.047$, $p = 0.95$, ANOVA). Thus, there were no significant differences in the average relative expression of *POMC* between samples obtained at ZT 2 (1.01 ± 0.43), ZT 10 (1.06 ± 0.38), nor at ZT 18 (1.09 ± 0.52) (Fig. 1c). This data suggests that *POMC* mRNA in the retina could have an ultradian (i.e. less than 24-h cycle) rhythm, possibly consisting of 8-h cycles of expression with peaks at ZT 2, 10 and 18 (Fig. 1d).

3.2. β-endorphin protein expression is regulated by circadian and light-driven mechanisms

In our original study of POMC and β-endorphin expression in the retina (Gallagher et al., 2010), we found that more cells expressed POMC-DsRed signal than β-endorphin. This could be explained by the POMC-DsRed signal being maintained even when β-endorphin is broken down and undetectable by immunohistochemistry, or by β-endorphin expression being rhythmic as it is in other rodent brain regions (Kerdelhue et al., 1983; Jamali and Tramu, 1999; Labrecque and Vanier, 1995). In this study, we tested the hypothesis that β-endorphin expression is dependent on light condition and/or circadian time-of-day using immunohistochemical experiments. In the mouse retina, β-endorphin is expressed by a subset of cholinergic amacrine cells (Gallagher et al., 2010), which can be reliably labeled by their expression of choline acetyltransferase (ChAT), the rate-limiting enzyme for acetylcholine synthesis. ChAT + cholinergic amacrine cells can be found in the inner

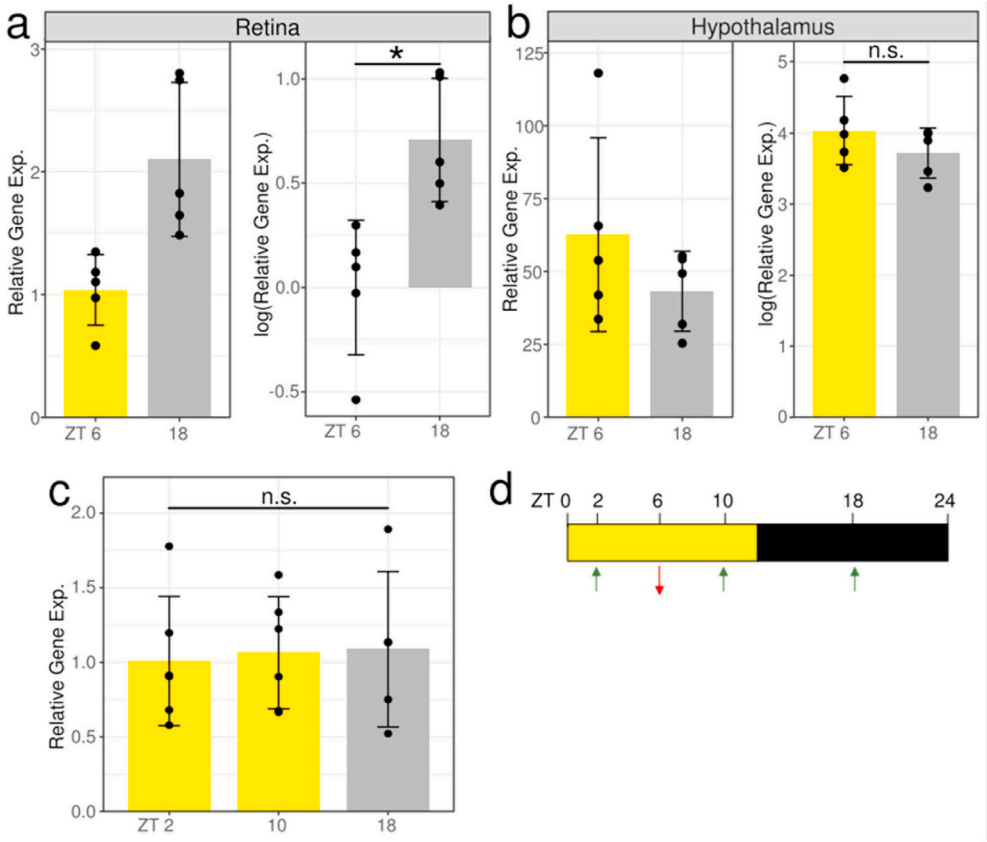

Fig. 1. ***POMC*** **mRNA in the retina appears to have cyclic variation across the day. (a, b)** Male WT mice were sacrificed in the middle of the light phase (Zeitgeber Time ZT 6, n = 5) or dark phase (ZT 18, n = 5). *POMC* mRNA in the retina and hypothalamus (relative to the reference gene *Tbp*)was measured by quantitative reverse-transcription PCR (qRT-PCR) with ZT 6 retinas as the control group. Relative gene expression values (left) were log transformed (right) to satisfy the assumptions of ANOVA. (**a**) *POMC* mRNA is significantly higher in the retinas of mice sacrificed at ZT 18 than ZT 6 (*p = 0.0082). (**b**) There was not a significant difference in hypothalamic *POMC* mRNA between ZT 6 and 18 (p = 0.1924). (**c**) *POMC* mRNA was quantified in WT retinas collected every 8 h (ZT 2 n = 6, ZT 10 n = 6, ZT 18 n = 5). The time of sacrifice was not a significant predictor of *POMC* expression (p = 0.95, ANOVA), and there were no significant differences in relative *POMC* expression in any of the three groups. All bars represent mean ± s.d. Yellow bars indicate light adaptation, while grey bars indicate dark adaptation. (**d**) Summary of results, where arrows indicate the relative expression of *POMC* mRNA at each timepoint. (For interpretation of the references to colour in this figure legend, the reader is referred to the Web version of this article.)

nuclear layer (INL) and ganglion cell layer (GCL) of the rodent retina (Voigt, 1986), with greater cell numbers in the INL (Whitney et al., 2008).

To assess whether β-endorphin expression in the retina is under circadian and/or light-driven regulation, we quantified the colocalization of β-endorphin immunolabeling with that of ChAT + somas in four conditions: light-adapted during the subjective day, dark-adapted during the subjective day, dark-adapted during the subjective night, and light-adapted during the subjective night (n = 3 mouse retinas/group; Fig. 2a, c). Representative images of β-endorphin and ChAT immunolabeling are shown in Fig. 3. We first confirmed that the average numbers of ChAT-immunopositive cells per mm^2 across the center and periphery regions of the INL and GCL (980 ± 206 and 842 ± 219, respectively) were comparable to previously published cholinergic

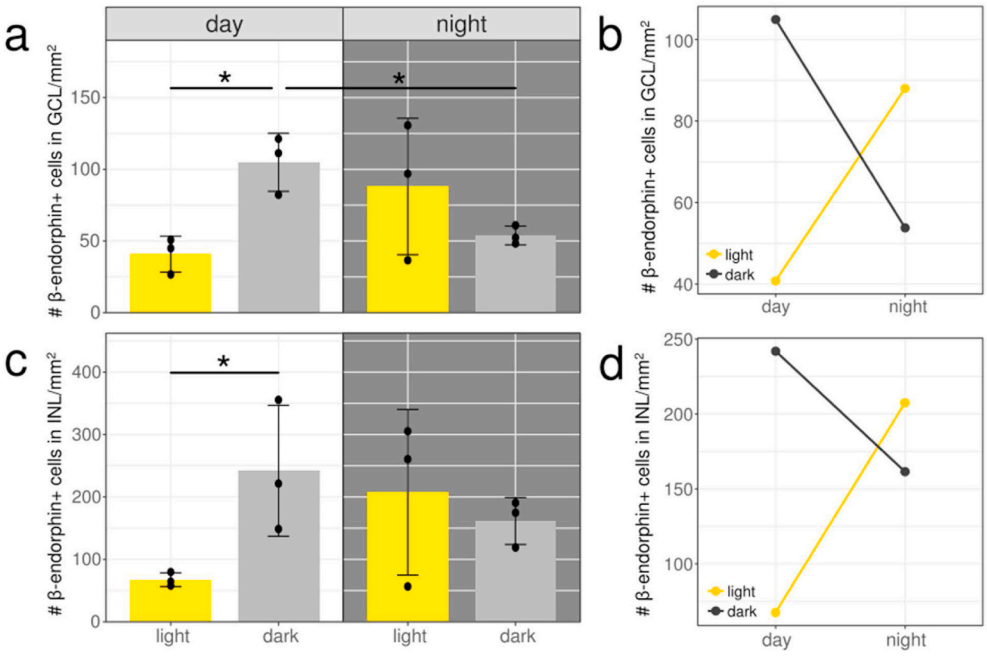

Fig. 2. β-endorphin expression in the mouse retina depends on both light condition and circadian time-of-day. (a, c) Points represent the number of β-endorphin-immunopositive ChAT + cells per square millimeter of the (**a**) ganglion cell layer (GCL) and (**c**) inner nuclear layer (INL) of each mouse retina (n = 3 per group). There were no significant differences in the number of ChAT + cells in the INL or GCL across all the groups (980 ± 206 and 842 ± 219, respectively). β-endorphin expression is most significantly increased when mice are dark-adapted for 2 h during the subjective day, but expression levels are generally higher in any samples that are dark-adapted and/or obtained in the subjective night. Bars represent mean ± s.d.* = p < 0.05 (**b, d**) The interaction of light and time influences β-endorphin expression in both the GCL (p = 0.013, **b**) and INL (p = 0.059, **d**). Dark-adaptation is associated with more β-endorphin + cells in the INL and GCL during the subjective day, but light-adaptation is associated with more β-endorphin + cells in the subjective night.

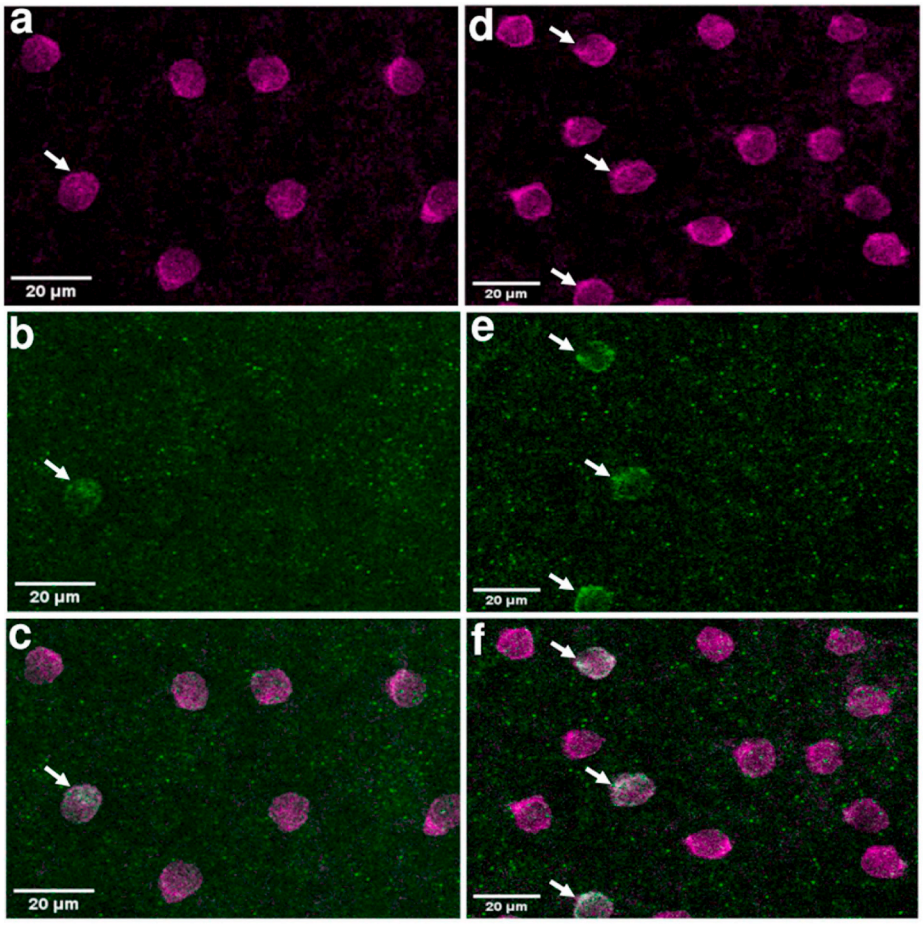

Fig. 3. Representative immunolabeling of choline acetyltransferase (ChAT) and β-endorphin in light- and dark-adapted retinas. Each image is a maximum projection of all z-stacks containing the cells in the imaged region. (**a**) ChAT expression in the inner nuclear layer (INL) of a light-adapted retina obtained in the daytime. (**b**) β-endorphin expression in the same retina as (**a**). (**c**) Merged composite of (**a**) and (**b**). (**d**) ChAT expression in the inner nuclear layer (INL) of a dark-adapted retina obtained in the daytime. (**e**) β-endorphin expression in the same retina as (**d**). (**f**) Merged composite of (**d**) and (**e**). Colocalization of magenta and green results in white; arrows indicate β-endorphin+/ChAT + cells. (For interpretation of the references to colour in this figure legend, the reader is referred to the Web version of this article.)

amacrine cell densities in C57BL/6J mice (Gallagher et al., 2010; Whitney et al., 2008; Zhang et al., 2005) and not significantly different between groups (Tables 2 and 3). Furthermore, the number of β-endorphin-immunopositive ChAT + cells per mm^2 in the INL and GCL of retinas that were light-adapted during the subjective day (67 ± 11 and 41 ± 13, respectively) were comparable to our original study on β-endorphin expression (Fernandez et al., 2016). The average percentage of ChAT + cells that expressed β-endorphin appeared to be lowest in mice that were light-adapted during the subjective day (ZT 4–8) in both the INL (7% versus 18–24%) and GCL (5% versus 7–12%). The average number of β-endorphin-immunopositive cells per mm^2 was higher in the INL (170 ± 101) than in the GCL (72 ± 35). We have included a representative video showing each optical section through the GCL, inner plexiform layer (IPL) and INL to demonstrate the quality of the whole-mount preparation and ChAT/β-endorphin labeling in each layer (Supp. Video 1).

The expression of β-endorphin in each group was compared using a multivariate ANOVA (MANOVA) with the number of β-endorphin + ChAT + cells per mm^2 of retina in the INL and GCL as two dependent variables, and time-of-day and light condition as independent variables. In this multivariate analysis, light condition and time-of-day were not significant predictors individually ($F_{2,7} = 0.75$, $p = 0.51$ and $F_{2,7} = 0.83$, $p = 0.48$, respectively), but the interaction of light condition and time-of-day was a significant predictor of the number of β-endorphin + ChAT + cells per mm^2 of retina ($F_{2,7} = 4.85$, $p = 0.048$). Thus, the number of β-endorphin + ChAT + cells per mm^2 is generally elevated in retinas that are dark-adapted and/or obtained during the subjective night (Fig. 2, Tables 2 and 3). We followed up our MANOVA analysis with individual univariate analyses for the INL and GCL. In the GCL, the interaction of light condition and time-of-day ($F_{1,8} = 10.05$, $p = 0.013$) was again a significant predictor, while light condition ($F_{1,8} = 0.93$, $p = 0.36$) and time-of-day ($F_{1,8} = 0.02$, $p = 0.9$) were not. The interaction

Table 2
Summary of ChAT and β-endorphin immunolabeling in the GCL.

Light Condition	Time of Day	n	Total ChAT + cells	Total β-endorphin + ChAT + cells	Average ChAT + cells/ mm^2	Average β-endorphin + ChAT + cells/mm^2
light	day	3	8795	413	779 ± 92	41 ± 13
light	night	3	12345	1191	909 ± 453	88 ± 48
dark	day	3	13001	1504	901 ± 121	105 ± 20
dark	night	3	11936	830	781 ± 109	54 ± 6

Table 3
Summary of ChAT and β-endorphin immunolabeling in the INL.

Light Condition	Time of Day	n	Total ChAT + cells	Total β-endorphin + ChAT + cells	Average ChAT + cells/ mm^2	Average β-endorphin + ChAT + cells/mm^2
light	day	3	10834	767	954 ± 123	67 ± 11
light	night	3	14180	2782	1029 ± 438	207 ± 133
dark	day	3	14630	3416	1008 ± 61	242 ± 105
dark	night	3	14103	2573	929 ± 116	161 ± 38

plot for β-endorphin expression in the GCL shows that while dark-adaptation is associated with more β-endorphin + ChAT + cells during the subjective day, light-adaptation is associated with more β-endorphin + ChAT + cells during the subjective night (Fig. 2b). Tukey-adjusted post-hoc comparisons revealed a significant increase in the average number of β-endorphin + ChAT + cells per mm^2 in the GCL (Table 2) in dark-adapted (105 ± 20) versus light-adapted retinas during the subjective day (41 ± 13; $t(8) = -2.92$, $p = 0.0192$) (Fig. 2a). Furthermore, β-endorphin expression was higher in dark-adapted retinas during the subjective day than during the subjective night (54 ± 6; $t(8) = 2.33$, $p = 0.0482$) (Fig. 2a). Lastly, the difference in the number of β-endorphin + cells between light-adapted retinas during the subjective night (88 ± 48) and the subjective day was slightly increased ($t(8) = -2.15$, $p = 0.06$) (Fig. 2a).

Interestingly, in the INL, neither light condition ($F_{1,8} = 1.64$, $p = 0.24$, ANOVA), time-of-day ($F_{1,8} = 0.35$, $p = 0.57$), nor the interaction of light condition and time-of-day ($F_{1,8} = 4.84$, $p = 0.059$) were statistically significant predictors of β-endorphin expression. However, we found that dark-adaptation is associated with increased β-endorphin expression during the subjective day in INL just as it is in the GCL (Fig. 2d). Moreover, light-adaptation during the subjective night, compared to dark-adaptation, is not as strongly associated with an increase in the number of β-endorphin + ChAT + cells in the INL as it is in the GCL, thus the expression of β-endorphin in the INL is relatively similar in both light conditions in the subjective night (Fig. 2d). Tukey-adjusted post-hoc comparisons revealed a significant increase in β-endorphin expression in dark-adapted (242 ± 105) versus light-adapted retinas during the subjective day (67 ± 11; $t(8) = 2.46$, $p = 0.0392$) (Table 3, Fig. 2c). Furthermore, there was a slight increase in the expression in light-adapted retinas during the subjective night (207 ± 133) compared to subjective day ($t(8) = -1.98$, $p = 0.0835$) (Fig. 2c).

In both the INL and GCL, the light-adapted samples obtained during the subjective day had the lowest average expression of β-endorphin. Changes to the light condition (i.e. dark-adaptation) and/or time-of-day (i.e. sacrificing mice at night) led to increases in the average number of ChAT + cells that express β-endorphin (Fig. 2). Notably, dark-adaptation during the subjective day resulted in the largest increase in β-endorphin expression. The expression of β-endorphin in samples obtained in the subjective night, regardless of light condition, tended to be higher than samples light-adapted during the subjective day, despite this difference not being statistically significant. The fact that the expression in dark-adapted samples obtained during the subjective night is not higher than in the subjective day is consistent with the circadian effect not being statistically significant. Overall, increased β-endorphin expression appears to be associated with acute dark adaptation during the subjective day, or sacrifice during the circadian night phase, periods when nocturnal mice should be active and awake.

3.3. Validation of the McKO mouse line

To test whether endogenous β-endorphin signaling via MORs expressed by ipRGCs influences the photoentrainment of circadian activity in nocturnal mice, we generated a mouse line wherein only ipRGCs lack functional MORs due to the cre-dependent deletion of exons 2 and 3 (McKO) (Cleymaet et al., 2021; Weibel et al., 2013). In order to validate this McKO mouse line, we used both qRT-PCR and RNAscope in situ hybridization. In our qRT-PCR experiments, we quantified *Oprm1* (MOR) mRNA expression in male and female WT (n=6) and McKO (n = 5) mice using primers that targeted the deleted region. *MOR* expression relative to the reference genes *Tbp* and *β-actin* was calculated using the average Cq values in the WT group as the control. Retinas from McKO animals had significantly lower *MOR* mRNA expression (0.33 ± 0.2) than retinas from WT mice (1.02 ± 0.2) ($t(8.604) = 5.88$, $p < 0.001$, T-test; Fig. 4a). This is consistent with the observation that, in the mouse retina, although MOR expression is not extensive, several cell types are labeled with the anti-MOR antibody, including Brn-3a positive putative ganglion cells, a few GAD67-expressing putative amacrine cells, and dopaminergic amacrine cells (Gallagher et al., 2012). Nonetheless, the present data indicates that MORs expressed by ipRGCs represent a major fraction of retinal MOR expression. Importantly, mice lacking functional MORs globally (MKO) were also generated by the deletion of exons 2 and 3 (Matthes et al., 1996), therefore they served as a negative control. Indeed, when we used the same *Oprm1* primers in these MKO mice (n = 5), we confirmed that there was no measurable amplification of *MOR* mRNA (data not shown). Furthermore, we quantified *MOR* mRNA in the hypothalamus and retina of WT and McKO mice and found no decrease in MOR expression in the hypothalamus of McKO mice (Supp. Fig. 2). Interestingly, MOR expression was approximately 15-fold higher in the hypothalamus than the retina ($t(7) = -44.412$, $p < 0.0001$; Supp. Fig. 2).

Using RNAscope in situ hybridization, we visualized melanopsin (*Opn4*) and MOR (*Oprm1*) mRNA (Fig. 4b1) in male and female WT (n =

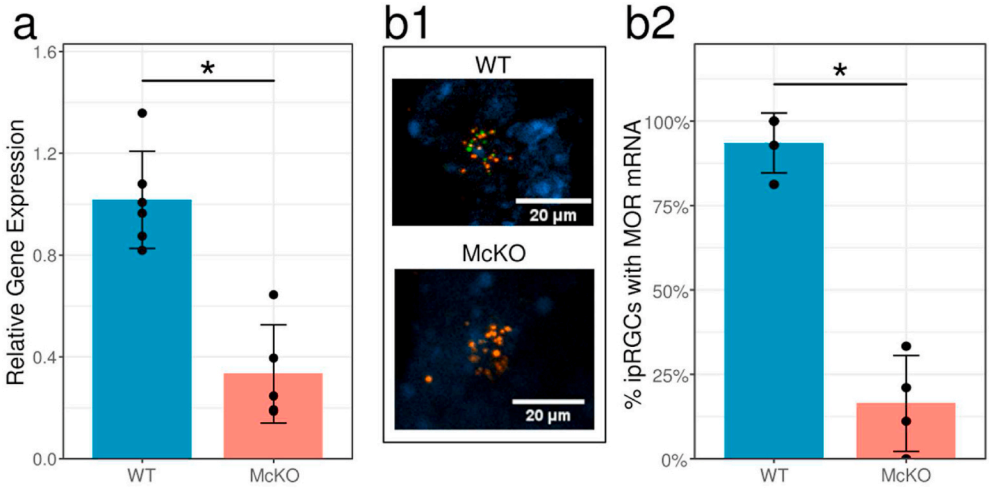

Fig. 4. Retinal μ-opioid receptor (MOR) mRNA expression is decreased in McKO mice compared to WT mice. McKO mice lack functional MORs only on intrinsically photosensitive retinal ganglion cells (ipRGCs) but retain functional MOR expression in other retinal cells. (**a**) MOR mRNA was measured in total retina extracts from WT (n = 6) and McKO (n = 5) mice by quantitative reverse transcription PCR (qRT-PCR). Expression was significantly lower in McKO mice (*$p < 0.001$). (**b1**) Representative images of RNAscope in situ hybridization used to fluorescently label melanopsin (*Opn4*) mRNA expressed by ipRGCs and MOR (*Oprm1*) mRNA. Images are average intensity projections of all z-stacks including these cells. *Opn4* mRNA was labeled with Opal 570 (orange), *Oprm1* mRNA with Opal 520 (green), and cell nuclei with DAPI (blue). (**b2**) Quantification of RNAscope in situ hybridization. Fewer ipRGCs express MOR mRNA in McKO mice (n = 4) compared to WT mice (n = 4) (*$p < 0.001$). Bars represent mean ± s.d. (For interpretation of the references to colour in this figure legend, the reader is referred to the Web version of this article.)

4) and McKO (n = 4) mice with probes that targeted exons 2 and 3 of *Oprm1*, the region deleted in the McKO mouse line and the same region targeted by our qRT-PCR primers. We found a statistically significant decrease in the percentage of *Opn4*+ cells (ipRGCs) that expressed *MOR* mRNA in McKO mice (16% ± 14%) compared to WT mice (94% ± 9%) (t(5.024) = −9.22, p = 0.00025, T-test; Fig. 4b2). In WT mice, the percentage of *Opn4*+ cells which expressed *MOR* mRNA ranged from 81.25% to 100%, while the percentage of *Opn4*+ cells which expressed *MOR* mRNA in McKO mice ranged from 0% to 33.3% (Fig. 4b2). Our observation that not all *Opn4*+ cells in WT mice express *MOR* mRNA is in line with our previous work on MOR immunoreactivity in ipRGCs. We showed MOR expression in M1-M3 ipRGC subtypes (Cleymaet et al., 2019), but whether M4-M6 subtypes express MORs is unknown (Schmidt et al., 2011; Quattrochi et al., 2019). Furthermore, an incomplete decrease in *MOR* mRNA has previously been shown in the exon 2 and 3-deletion model (Weibel et al., 2013; Severino et al., 2020), and while *MOR* mRNA transcripts lacking exons 2 and 3 may still be transcribed, the coding sequence for the protein is disrupted and the receptor is therefore non-functional (Matthes et al., 1996).

3.4. Endogenous activation of MORs expressed by ipRGCs modulates activity in the dark

In order to determine the contribution of MORs expressed by ipRGCs on the photoentrainment of activity cycles, the x-y movement of male WT (n = 9) and McKO (n = 7) mice was measured by surgically implanted mini-telemetry transmitters (DSI). Each minute, movement (activity) was measured in arbitrary units (a.u.), and the activity measurements from each mouse were then averaged over at least 4 consecutive days (Fig. 5). Mice were considered inactive if no x-y movement was recorded for the entire minute. Bouts of inactivity (i.e. no x-y movement) lasting longer than 40 s are an excellent approximation of sleep, as they show high agreement with estimates of sleep obtained by EEG and EMG recordings (Pack et al., 2007; Fisher et al., 2012). Using longer bouts of inactivity (e.g. 1 min as here) may underestimate sleep amounts (Pack et al., 2007).

The activity data was analyzed using a linear mixed model with activity or inactivity as the response variable, and genotype and phase as predictor variables grouped by the mouse ID. As expected for nocturnal animals, WT mice displayed more activity in the dark phase (0.18 ± 0.04) than in the light phase (0.06 ± 0.02; t(14) = −7.837, $p < 0.0001$, Tukey-adjusted comparisons) (Fig. 5a and b). Conversely, they spent more time inactive in the light phase (64% ± 6%) than in the dark phase (34% ± 7%; t(14) = 8.081, $p < 0.0001$) (Fig. 5c and d). We found that McKO mice retained nocturnal circadian behavior, with higher activity in the dark phase (0.12 ± 0.05) compared to the light phase (0.05 ± 0.03; t(14) = −3.892, p = 0.0016) (Fig. 5a and b). Accordingly, they spent more time inactive in the light phase (65% ± 8%) than in the dark phase (46% ± 11%; t(14) = 4.618, p = 0.0004) (Fig. 5c and d). Furthermore, the overall pattern of activity/inactivity was similar in both WT and McKO mice, as the onset of activity occurred approximately 30 min before the dark phase began in both groups (Fig. 5a, c).

Despite the preservation of nocturnal circadian behavior, McKO mice were significantly less active (0.12 ± 0.05) than WT mice (0.18 ± 0.04) in the dark phase (t(27.2) = −3.459, p = 0.0018; Fig. 5b). Accordingly, McKO mice displayed higher levels of inactivity (46% ± 11%) than WT mice (34% ± 7%) in the dark phase (t(28) = 2.871, p = 0.0077). Interestingly, in the light phase, there were no significant differences in activity (t(27.2) = −0.55, p = 0.5868) nor inactivity (t(28) = 0.222, p = 0.8347; Fig. 5d), suggesting MORs expressed by ipRGCs might play a more important role in modulating nocturnal activity in the dark.

3.5. Endogenous activation of MORs expressed by ipRGCs modulates healthy sleep/wake

Although inactivity lasting longer than 40 s can approximate sleep (Pack et al., 2007; Fisher et al., 2012), we wanted to perform a more detailed analysis of sleep architecture to determine the contribution of MORs expressed by ipRGCs on the photoentrainment of sleep/wake activity. Male WT (n = 10) and McKO (n = 9) mice were implanted with

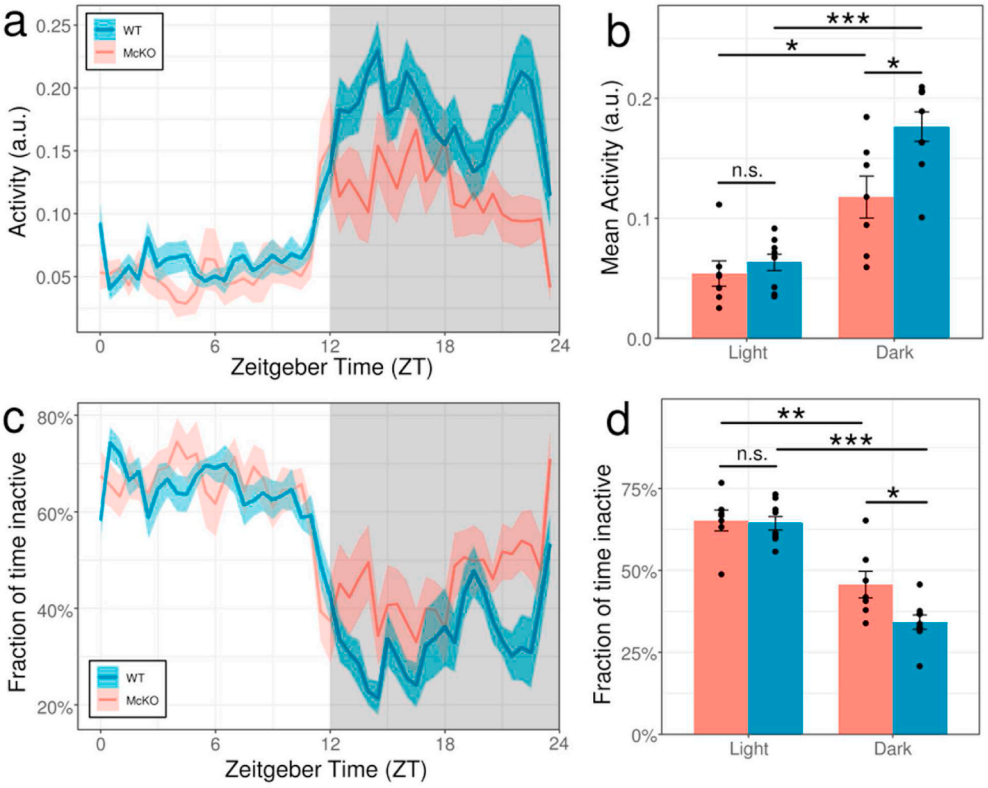

Fig. 5. McKO mice are less active in the dark phase than WT mice but retain nocturnal circadian behavior. (a) Average activity (x-y movement) of all WT (n = 9) and McKO (n = 7) mice over 24 h, averaged from recordings across at least 4 days. (**b**) Quantification of the average activity of each individual mouse in the light and dark phases. (**c**) Average fraction of time all WT and McKO mice spent inactive (i.e. no x-y movement for 1 min) over 24 h, averaged from recordings across at least 4 days. (**d**) Quantification of the average fraction of time each individual mouse spent inactive in the light and dark phases. Bars represent mean ± s.e.* = $p < 0.01$, ** = $p < 0.001$, *** = $p < 0.0001$.

telemetry transmitters (DSI) that recorded EEG and EMG as well as x-y movement activity for at least 3 consecutive days. These data were used to classify behavior into 10-s periods of wake, slow-wave sleep (SWS) or paradoxical (REM) sleep. The amount of time in each stage was totaled and averaged across all recorded days. The amount of artifact was less than 1% of the recorded time for all mice.

The sleep data was analyzed using a linear mixed model with the amount of wake, SWS, or REM sleep as the response variable, and genotype and phase as predictor variables grouped by the mouse ID. As in our activity analysis, our sleep/wake analysis showed that McKO mice retain nocturnal circadian sleep/wake behavior. McKO mice display more wakefulness in the dark phase (54.6% ± 7%) compared to the light phase (22.4% ± 3.5%; t(435) = 15.043, $p < 0.0001$, Tukey-adjusted comparisons), just as WT mice do (56% ± 4.1% and 26.8% ± 3.6%; t (435) = 14.387, $p < 0.0001$) (Fig. 6a). Furthermore, McKO mice display more SWS during the light phase (70.4% ± 5.8%) than the dark phase (41.4% ± 7%; t(435) = −14.571, $p < 0.0001$), as do WT mice (65.5% ± 7% and 39.2% ± 5.6%; t(435) = −13.93, $p < 0.0001$). The same pattern is found in REM sleep, wherein levels in McKO mice are higher in the light phase (7.2% ± 3.5%) compared to the dark phase (3.8% ± 1.8%; t (435) = −9.535, $p < 0.0001$), just as they are in the WT mice (7.4% ± 4% and 4.4% ± 2%; t(435) = −9.375, $p < 0.0001$).

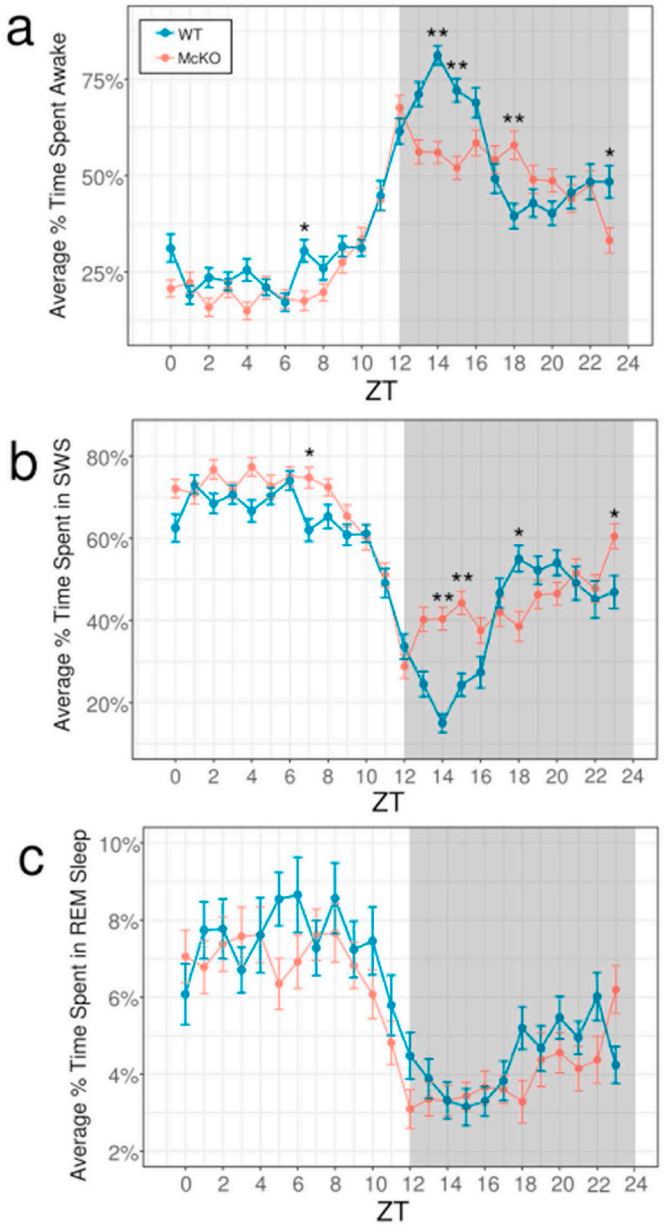

Fig. 6. McKO mice have reduced wakefulness and increased slow-wave sleep (SWS) compared to WT mice. Sleep/wake architecture based on activity, EEG and EMG recordings from WT (n = 10) and McKO mice (n = 9) averaged over at least 3 consecutive days. Average percent of time mice spent (**a**) awake, in (**b**) SWS, and (**c**) REM sleep. Grey box indicates the dark phase. Error bars represent mean ± s.e. * = $p < 0.05$,** = $p < 0.01$.

Across the 24-h day, we found no significant differences between McKO and WT mice in the median amount of wake (37.2% and 40.1%, respectively; Z = 0.38, $p = 0.2427$), REM sleep (5.9% and 4.3%, respectively; Z = 0.24, $p = 0.4598$), nor SWS (57.9% and 53.4%, respectively; Z = 0.47, $p = 0.1447$) using the non-parametric Wilcoxon rank-sum test. However, when analyzing the average amount of wakefulness in each phase by ANOVA, we found that McKO mice spent less time awake (22.4% ± 3.5%) than WT mice (26.8% ± 3.6%) in the light phase (t(56.7) = −2.038, $p = 0.0463$, Tukey-adjusted comparisons), but not in the dark phase (54.6% ± 7% and 56% ± 4.1%, respectively; t (56.7) = -0.67, $p = 0.51$; Fig. 6a). Accordingly, there was a slight increase in the amount of SWS in the light phase in McKO (70.4% ± 5.8%) compared to WT mice (65.5% ± 7%; t(29.1) = 1.733, $p = 0.0937$), but not in the dark phase (42.4% ± 7% and 39.2% ± 5.6%, respectively; t (29.1) = 0.774, $p = 0.4451$; Fig. 6b). Despite no significant differences across the entire dark phase, we found differences in wakefulness and SWS at the level of individual ZTs (Fig. 6a and b). Most strikingly, in the dark phase, WT mice experienced a peak in wakefulness of about 81% (ZT 14), while the peak of wakefulness in McKO mice only reached 68% (ZT 12; Fig. 6a). Furthermore, the lowest amount of SWS in 1 ZT h was much lower in WT mice (15% at ZT 14) than in McKO mice (29% at ZT 12; Fig. 6b). Interestingly, we did not detect any differences in REM sleep between genotypes in either phase or at any ZT (Fig. 6c).

A detailed analysis of the number and average length of sleep/wake bouts per day in each phase revealed no significant differences between McKO and WT mice (Supp. Fig. 3). Together, these data suggest that McKO mice retain relatively normal nocturnal sleep/wake architecture but do exhibit lower levels of wakefulness compared to WT mice in the light phase and at several time points in the dark phase, which may be related to increased levels of SWS, but not REM sleep.

4. Discussion

4.1. Regulation of POMC and β-endorphin expression in the mouse retina

Studies have suggested that *POMC* mRNA is more highly expressed in the rodent brain at night, with most work focusing on the arcuate nucleus (Agapito et al., 2014; Chen et al., 2004; Steiner et al., 1994). Other studies, especially those which measured POMC in the whole rodent hypothalamus, including ours, have failed to uncover such cyclic variation (Xu et al., 1999; St ü tz et al., 2007; Lu et al., 2002). This may be consistent with the notion that POMC expression is region-specific (Bicknell, 2008), and thus cyclic variation in particular hypothalamic regions could be masked when using the whole tissue. Furthermore, our data suggests that *POMC* mRNA in the mouse retina might have an ultradian rhythm that peaks in expression every 8 h. Ultradian gene expression, especially with periods of ~8 h, may be more common than previously thought, but documenting ultradian rhythms is complicated by the need for frequent sampling and the fact that genes can have both circadian and ultradian expression patterns (van der Veen and Gerkema, 2017; Ono et al., 2015).

While cyclic variation in *POMC* mRNA may be sufficient to drive circadian β-endorphin expression, post-transcriptional regulation is also thought to be critical to the production of circadian proteins and several mechanisms have been proposed, particularly the activity of RNA-binding proteins and microRNAs (Reddy et al., 2006; Chiang et al., 2014; Kojima et al., 2011). The mechanisms underlying rhythmic POMC processing and light-driven β-endorphin expression in the retina may

also involve changes in the expression and/or activity of the enzymes that cleave POMC into β-endorphin, including prohormone convertase 1/3 (PC1/3), PC2, and Yapsin A (Cawley et al., 2016). Expression of PC1/3 and PC2 in the human retina has been demonstrated (Fuller et al., 2009), but we are not aware of any reports confirming Yapsin A expression in the retina. Future studies will examine the circadian expression of these enzymes in the mammalian retina.

4.2. Role of β-endorphin in sleep

The findings presented in this study implicate retinal β-endorphin in modulating sleep/wake behavior via activation of MORs expressed by ipRGCs in the dark. Most β-endorphin + cells in the retina are ChAT+ (~80%) and since the identities of the other β-endorphin-expressing in the mouse retina have not been elucidated (Gallagher et al., 2010), they were not quantified here. Future studies should characterize all β-endorphin-expressing cell types in the mouse retina and determine whether circadian timing and/or light condition also affects β-endorphin expression in these populations. Furthermore, while we cannot exclude that retinal β-endorphin also exerts neuromodulatory effects on other MOR-expressing cells in the retina, the behavioral data from our McKO mouse line implicates the activation of MORs expressed by ipRGCs in contributing to the modulation of sleep/wake cycles in mice. We propose this may occur via altered signaling in the photoentrainment pathway (i.e. ipRGCs projecting to the SCN and sleep/wake centers such as the preoptic area).

Increased retinal β-endorphin expression during the active (i.e. dark) phase of nocturnal mice appears to coincide with the existing body of literature regarding β-endorphin's role in sleep/wake behavior (Pilozzi et al., 2021). Early studies showed intraventricular injection of β-endorphin led to increased arousal in cats (King et al., 1981) and rats (Riou et al., 1982). In rats, sleep deprivation is associated with increased plasma β-endorphin levels (Przewlocka et al., 1986), and administration of β-endorphin increases the latency to sleep while MOR-selective antagonist naloxone reduces sleep latency (Fratta et al., 1987). In humans, β-endorphin levels are elevated in the cerebral spinal fluid of children with sleep apnea, and the opioid receptor antagonist naltrexone is an effective treatment (Myer et al., 1990).

Despite evidence that β-endorphin acting on MORs is associated with changes in sleep/wake activity in model organisms as well as humans, how endogenous β-endorphin may modulate sleep/wake behavior is not currently well understood. The data presented in this study implicate β-endorphin in modulating natural sleep/wake processes via the activation of MORs expressed by ipRGCs. We propose that increased β-endorphin expression in the dark may inhibit the spontaneous firing activity of ipRGCs (Zhao et al., 2014) through increased endogenous activation of MORs (Cleymaet et al., 2019) in order to promote wakefulness in the nocturnal mouse.

4.3. Activity vs. sleep/wake measurements

Our activity and sleep/wake analyses provided similar, though not identical, results. In general, we found that McKO mice exhibited less activity/wakefulness and more inactivity/SWS compared to WT mice. In our activity analysis, we found that McKO mice were less active than WT mice in the dark phase. Although we did not detect any differences in average wakefulness across the dark phase in our sleep/wake analysis, we found a significant decrease in the peak in wakefulness at the beginning of the dark phase in McKO mice compared to WT mice, which is consistent with our activity data.

Scoring activity based on x-y movement is limited due to its inability to measure movements such as scratching, grooming, and sniffing, where the mouse is awake but not moving around the cage. Additionally, while bouts of inactivity longer than 40s are a good approximation of sleep in mice, bouts of 60 s as used here may underestimate sleep (Pack et al., 2007; Fisher et al., 2012). Conversely, scoring wakefulness not only based on activity but also EEG and EMG recordings provides a nuanced and precise determination of sleep/wake state (e.g. SWS or REM) as well as precise calculations of bout length. Thus, while our activity analysis only uncovered a difference between McKO and WT mice in the dark phase, our sleep/wake analysis uncovered differences in both the light and dark phases. Importantly, this analysis revealed that changes in McKO sleep/wake behavior may stem from changes in SWS, but not REM sleep. It is worth noting that our sleep analysis, like our activity analysis, is limited in its ability to quantify stationary behavior. Thus while increased SWS contributes to the decreased activity in McKO mice, changes to stationary or anxiety behavior may also play a role.

4.4. Proposed mechanism of MORs expressed by ipRGCs modulating sleep/wake behavior

Light-evoked ipRGC firing activity (Berson, 2003) is known to induce sleep in nocturnal mice, while exposure to darkness induces wakefulness in an ipRGC-dependent manner (Altimus et al., 2008). It has been theorized that ipRGCs continuously signal the presence of light to the brain in the absence of a repression of signaling (Altimus et al., 2008; Schmidt et al., 2011). This could be supported by evidence that ipRGCs exhibit spontaneous activity in the dark (Zhao et al., 2014) and their membrane potential in the dark is near their spike threshold (i.e. the small depolarization caused by the adsorption of a single photon can increase their spiking rate several-fold) (Do et al., 2009). Thus, endogenous activation of the MORs expressed by ipRGCs in the dark, when mice should be awake, may serve to inhibit spontaneous ipRGC firing. In doing so, it might prevent ipRGC spiking activity which would otherwise be interpreted by the brain as a signal for light and therefore prevent the induction and maintenance of sleep.

The firing activity of ipRGCs is directly communicated to the suprachiasmatic nucleus (SCN), the master regulator of circadian rhythms, via the retinohypothalamic tract (RHT). Light stimulates neurotransmitter release through the RHT to the SCN and increases the firing rate of SCN neurons in both nocturnal and diurnal organisms, although the behavioral responses to SCN activation (i.e. sleep or wake) differ (Hastings et al., 2018). Photoentrainment, the alignment of circadian sleep/wake cycles to environmental light/dark cycles, requires ipRGC innervation to the SCN (Güler et al., 2008). Circadian rhythms in the SCN are thought to be maintained by cells in the eye - presumably ipRGCs due to their direct projections to the SCN (Fernandez et al., 2016) - even in the absence of light (Lee et al., 2003). This supports our assertion that, in the dark, inhibition of ipRGC firing via activation of their MORs could contribute to circadian rhythms of sleep/wake activity.

Furthermore, modulation of ipRGC activity by β-endorphin activating MORs expressed by ipRGCs may also influence sleep/wake activity through projections to the preoptic area (POA), including the ventrolateral preoptic nucleus (VLPO). Although the ipRGC-SCN circuit is necessary for circadian regulation of sleep/wake, it is not sufficient to induce sleep in response to acute light (Rupp et al., 2019). Recent work showed that ipRGCs, specifically the M1 subtype that comprises most of the input to the SCN (Baver et al., 2008), innervate the POA to a greater extent than previously thought (Zhang et al., 2021). Chemogenetic activation of this ipRGC-POA circuit led to an increase in acute light-induced non-rapid eye movement (NREM) sleep, but interestingly, did not affect REM sleep (Zhang et al., 2021). Conversely, inhibition of the ipRGC-POA circuit inhibits NREM, not but REM, sleep (Zhang et al., 2021). Accordingly, the light-responsive POA neurons necessary for light-induced NREM sleep project to brain regions known to be involved in wakefulness, such as the lateral hypothalamus, but not to regions that promote or suppress REM sleep, such as the pedunculopontine nucleus or locus coeruleus, respectively (Scammell et al., 2017; Zhang et al., 2021).

Moreover, the VLPO receives input from both ipRGCs and the SCN

(LeGates et al., 2014), and VLPO neurons are sometimes referred to as a sleep switch, wherein activation of sleep-promoting VLPO neurons (Sherin et al., 1996) leads to sleep while inhibition of VLPO neurons by wake-active orexin neurons leads to wakefulness (Fuller et al., 2006; Saper et al., 2001). Then, it is tempting to speculate that McKO mice lacking MORs expressed by ipRGCs have less inhibition of ipRGC activity (and therefore less inhibition of VLPO neurons), which may explain the decreased wakefulness we see in these mice. Together, this body of literature suggests that inhibition of ipRGC activity in the dark, by β-endorphin activating MORs expressed by ipRGCs, may be important for inhibiting SCN neurons and sleep-promoting VLPO to lead to wakefulness. Since ipRGCs project to brain regions involved in the regulation of both circadian (e.g. SCN) and acute light-induced (e.g. VLPO) sleep to coordinate photoentrainment, the alterations to sleep/-wake behavior in McKO mice might be underscored by changes in multiple ipRGC projection areas.

4.5. The effect of opioid drugs on sleep/wake

Both acute and chronic opioid use produce sleep disturbances, which are associated with negative outcomes like depression and increased risk of relapse and dependence (Tripathi et al., 2020; Huhn and Finan, 2021). Sleep disturbances have recently emerged as an important, yet understudied, therapeutic target for improving outcomes for individuals on long-term opioid therapy and medications for opioid use disorder (e.g. methadone) (Huhn and Finan, 2021). Although opioids like morphine have been used for millennia (Brownstein, 1993), the mechanism by which sleep disturbances occur is not well understood (Tripathi et al., 2020). It is possible that a single opioid dose may have distinct effects from chronic dosing, as is the case with pupillary light reflex (Grace et al., 2010). Acute morphine treatment is thought to promote wakefulness in rats by inhibiting the sleep-promoting neurons of the VLPO (Wang et al., 2013). This mechanism, however, may not explain the persistent and progressive sleep disturbances associated with long-term opioid use.

Long-term opioid users sleep and wake at inappropriate times of day (i.e. insomnia and daytime sleepiness) (Zgierska et al., 2007), which suggests alterations to photoentrainment. Photoentrainment is exclusively mediated by ipRGCs (Güler et al., 2008), which reside in the ganglion cell layer of the retina in contact with the vitreous humor. It is known that opioid metabolites deposit in the vitreous humor of the human eye post-mortem (Wyman and Bultman, 2004; Fernández et al., 2013), and that most opioid drugs exert their effects through MORs (Raynor et al., 1993). As such, the ability of β-endorphin to modulate the photoentrainment of sleep/wake rhythms by activating the MORs expressed by ipRGCs might be disrupted by the deposition of opioid metabolites in the vitreous humor. Moreover, morphine administration in mice abolishes the circadian rhythm of β-endorphin release into the plasma that occurs in response to pain (Rasmussen and Farr, 2003). Therefore, morphine might be able to abolish the rhythmicity of retinal β-endorphin release, thus altering the natural rhythm of sleep/wake cycle modulation by ipRGCs. It is tempting to speculate that if the novel endogenous opioid pathway discussed here is present in human retinas, then one or another of these mechanisms could contribute to opioid-induced sleep disturbances.

5. Conclusions

The major conclusions of this study are as follows: in the mouse retina, (1) mRNA expression of β-endorphin's precursor *POMC* appears to have a cyclic rhythm, (2) β-endorphin expression is regulated by light-driven and circadian mechanisms such that expression increases in the dark and/or in the subjective night when mice are active, and (3) endogenous opioid signaling through μ-opioid receptors on ipRGCs, perhaps driven by β-endorphin, plays a modulatory role in establishing healthy sleep/wake cycles. This final point was determined using mice with a cell-specific knockout of functional MORs expressed by ipRGCs (McKO). A detailed analysis of sleep architecture showed that McKO mice were awake for less time in both the light and dark phases, and this was associated with an increase in the amount of slow-wave sleep but not paradoxical/rapid eye movement (REM) sleep.

CRediT authorship contribution statement

Casey-Tyler Berezin: Conceptualization, Data curation, Formal analysis, Funding acquisition, Investigation, Methodology, Project administration, Software, Supervision, Validation, Visualization, Writing – original draft, Writing – review & editing. **Nikolas Bergum:** Data curation, Formal analysis, Methodology, Software, Investigation, Visualization, Writing – review & editing. **Kes A. Luchini:** Formal analysis, Validation, Writing – review & editing. **Sierra Curdts:** Formal analysis, Methodology, Software, Validation, Writing – review & editing. **Christian Korkis:** Methodology, Investigation, Writing – review & editing. **Jozsef Vigh:** Conceptualization, Data curation, Funding acquisition, Methodology, Project administration, Supervision, Writing – review & editing.

Declaration of competing interest

The Authors declare no conflict of interest.

Data availability

Data will be made available on request (https://github.com/ctberezin/Vigh-manu1).

Acknowledgements

We thank Connie M. King for her assistance with the transmitter implantation surgeries. We thank Susan M. Bailey and Lynn E. Taylor for access to and assistance with the qRT-PCR detection system. Funding for this work was provided by grants from the National Eye Institute (NEI) EY029227-01A1 (J.V.) and the National Institutes of Health (NIH) T32GM132057 (C.-T.B.). The funding sources had no involvement in study design, data collection/analysis, nor in writing/publication.

Appendix A. Supplementary data

Supplementary data to this article can be found online at https://doi.org/10.1016/j.nbscr.2022.100078.

References

Adachi, H., Tominaga, H., Maruyama, Y., et al., 2015. Stage-specific reference genes significant for quantitative PCR during mouse retinal development. Gene Cell. 20 (8), 625–635. https://doi.org/10.1111/gtc.12254.

Agapito, M.A., Zhang, C., Murugan, S., Sarkar, D.K., 2014. Fetal alcohol exposure disrupts metabolic signaling in hypothalamic proopiomelanocortin neurons via a circadian mechanism in male mice. Endocrinology 155 (7), 2578–2588. https://doi.org/10.1210/en.2013-2030.

Altimus, C.M., Guler, A.D., Villa, K.L., McNeill, D.S., LeGates, T.A., Hattar, S., 2008. Rods-cones and melanopsin detect light and dark to modulate sleep independent of image formation. Proc. Natl. Acad. Sci. USA 105 (50), 19998–20003. https://doi.org/10.1073/pnas.0808312105.

Altschuler, R.A., Mosinger, J.L., Hoffman, D.W., Parakkal, M.H., 1982. Immunocytochemical localization of enkephalin-like immunoreactivity in the retina of the Guinea pig. Proc. Natl. Acad. Sci. USA 79 (7), 2398–2400. https://doi.org/10.1073/pnas.79.7.2398.

Baver, S.B., Pickard, G.E., Sollars, P.J., Pickard, G.E., 2008. Two types of melanopsin retinal ganglion cell differentially innervate the hypothalamic suprachiasmatic nucleus and the olivary pretectal nucleus. Eur. J. Neurosci. 27 (7), 1763–1770. https://doi.org/10.1111/j.1460-9568.2008.06149.x.

Beier, C., Zhang, Z., Yurgel, M., Hattar, S., 2021. Projections of ipRGCs and conventional RGCs to retinorecipient brain nuclei. J. Comp. Neurol. 529 (8), 1863–1875. https://doi.org/10.1002/cne.25061.

Berson, D.M., 2003. Strange vision: ganglion cells as circadian photoreceptors. Trends Neurosci. 26 (6), 314–320. https://doi.org/10.1016/S0166-2236(03)00130-9.

Bicknell, A.B., 2008. The tissue-specific processing of pro-opiomelanocortin. J. Neuroendocrinol. 20 (6), 692–699. https://doi.org/10.1111/j.1365-2826.2008.01709.x.
Borbe, H.O., Wollert, U., Müller, W.E., 1982. Stereospecific [3H]naloxone binding associated with opiate receptors in bovine retina. Exp. Eye Res. 34 (4), 539–544. https://doi.org/10.1016/0014-4835(82)90026-4.
Borniger, J.C., Weil, Z.M., Zhang, N., Nelson, R.J., 2013. Dim light at night does not disrupt timing or quality of sleep in mice. Chronobiol. Int. 30 (8), 1016–1023. https://doi.org/10.3109/07420528.2013.803196.
Brownstein, M.J., 1993. A brief history of opiates, opioid peptides, and opioid receptors. Proc. Natl. Acad. Sci. USA 90 (12), 5391–5393. https://doi.org/10.1073/pnas.90.12.5391.
Burbach, J.P.H., 2010. Neuropeptides from concept to online database www.neuropeptides.nl. Eur. J. Pharmacol. 626 (1), 27–48. https://doi.org/10.1016/j.ejphar.2009.10.015.
Cawley, N.X., Li, Z., Loh, Y.P., 2016. 60 years of POMC: biosynthesis, trafficking, and secretion of pro-opiomelanocortin-derived peptides. J. Mol. Endocrinol. 56 (4), T77–T97. https://doi.org/10.1530/JME-15-0323.
Chen, C.P., Kuhn, P., Advis, J.P., Sarkar, D.K., 2004. Chronic ethanol consumption impairs the circadian rhythm of pro-opiomelanocortin and period genes mRNA expression in the hypothalamus of the male rat: alcohol effects on hypothalamic clocks. J. Neurochem. 88 (6), 1547–1554. https://doi.org/10.1046/j.1471-4159.2003.02300.x.
Chiang, C.K., Mehta, N., Patel, A., et al., 2014. In: Kramer, A. (Ed.), The Proteomic Landscape of the Suprachiasmatic Nucleus Clock Reveals Large-Scale Coordination of Key Biological Processes, vol. 10. PLoS Genet, e1004695. https://doi.org/10.1371/journal.pgen.1004695, 10.
Cleymaet, A.M., Gallagher, S.K., Tooker, R.E., et al., 2019. μ-Opioid receptor activation directly modulates intrinsically photosensitive retinal ganglion cells. Neuroscience 408, 400–417. https://doi.org/10.1016/j.neuroscience.2019.04.005.
Cleymaet, A.M., Berezin, C.T., Vigh, J., 2021. Endogenous opioid signaling in the mouse retina modulates pupillary light reflex. Int. J. Mol. Sci. 22 (2), 554. https://doi.org/10.3390/ijms22020554.
Czeisler, C.A., Shanahan, T.L., Klerman, E.B., et al., 1995. Suppression of melatonin secretion in some blind patients by exposure to bright light. N. Engl. J. Med. 332 (1), 6–11. https://doi.org/10.1056/NEJM199501053320102.
Do, M.T.H., Kang, S.H., Xue, T., et al., 2009. Photon capture and signalling by melanopsin retinal ganglion cells. Nature 457 (7227), 281–287. https://doi.org/10.1038/nature07682.
Fernández, P., Seoane, S., Vázquez, C., Tabernero, M.J., Carro, A.M., Lorenzo, R.A., 2013. Chromatographic determination of drugs of abuse in vitreous humor using solid-phase extraction: chromatographic determination of drugs of abuse in vitreous humor. J. Appl. Toxicol. 33 (8), 740–745. https://doi.org/10.1002/jat.2722.
Fernandez, D.C., Chang, Y.T., Hattar, S., Chen, S.K., 2016. Architecture of retinal projections to the central circadian pacemaker. Proc. Natl. Acad. Sci. USA 113 (21), 6047–6052. https://doi.org/10.1073/pnas.1523629113.
Fisher, S.P., Godinho, S.I.H., Pothecary, C.A., Hankins, M.W., Foster, R.G., Peirson, S.N., 2012. Rapid assessment of sleep/wake behaviour in mice. J. Biol. Rhythm. 27 (1), 48–58. https://doi.org/10.1177/0748730411431550.
Fratta, W., Collu, M., Martellotta, M.C., Pichiri, M., Muntoni, F., Gessa, G.L., 1987. Stress-induced insomnia: opioid-dopamine interactions. Eur. J. Pharmacol. 142 (3), 437–440. https://doi.org/10.1016/0014-2999(87)90084-7.
Freedman, M.S., Lucas, R.J., Soni, B., et al., 1999. Regulation of mammalian circadian behavior by non-rod, non-cone, ocular photoreceptors. Science 284 (5413), 502–504. https://doi.org/10.1126/science.284.5413.502.
Fuller, P.M., Gooley, J.J., Saper, C.B., 2006. Neurobiology of the sleep-wake cycle: sleep architecture, circadian regulation, and regulatory feedback. J. Biol. Rhythm. 21 (6), 482–493. https://doi.org/10.1177/0748730406294627.
Fuller, J.A., Brun-Zinkernagel, A.M., Clark, A.F., Wordinger, R.J., 2009. Subtilisin-like proprotein convertase expression, localization, and activity in the human retina and optic nerve head. Invest. Ophthalmol. Vis. Sci. 50 (12), 5759–5768. https://doi.org/10.1167/iovs.08-2616.
Güler, A.D., Ecker, J.L., Lall, G.S., et al., 2008. Melanopsin cells are the principal conduits for rod–cone input to non-image-forming vision. Nature 453 (7191), 102–105. https://doi.org/10.1038/nature06829.
Gallagher, S.K., Witkovsky, P., Roux, M.J., et al., 2010. β-Endorphin expression in the mouse retina. J. Comp. Neurol. 518 (15), 3130–3148. https://doi.org/10.1002/cne.22387.
Gallagher, S.K., Anglen, J.N., Mower, J.M., Vigh, J., 2012. Dopaminergic amacrine cells express opioid receptors in the mouse retina. Vis. Neurosci. 29 (3), 203–209. https://doi.org/10.1017/S0952523812000156.
Geissmann, Q., Rodriguez, L.G., Beckwith, E.J., Gilestro, G.F., 2019. Rethomics: an R framework to analyse high-throughput behavioural data. PLoS One 14 (1), e0209331. https://doi.org/10.1371/journal.pone.0209331.
Grace, P.M., Stanford, T., Gentgall, M., Rolan, P.E., 2010. Utility of saccadic eye movement analysis as an objective biomarker to detect the sedative interaction between opioids and sleep deprivation in opioid-naive and opioid-tolerant populations. J. Psychopharmacol. 24 (11), 1631–1640. https://doi.org/10.1177/0269881109352704.
Hastings, M.H., Maywood, E.S., Brancaccio, M., 2018. Generation of circadian rhythms in the suprachiasmatic nucleus. Nat. Rev. Neurosci. 19 (8), 453–469. https://doi.org/10.1038/s41583-018-0026-z.
Hattar, S., Kumar, M., Park, A., et al., 2006. Central projections of melanopsin-expressing retinal ganglion cells in the mouse. J. Comp. Neurol. 497 (3), 326–349. https://doi.org/10.1002/cne.20970.
Hellemans, J., Mortier, G., De Paepe, A., Speleman, F., Vandesompele, J., 2007. qBase relative quantification framework and software for management and automated analysis of real-time quantitative PCR data. Genome Biol. 8 (2), R19. https://doi.org/10.1186/gb-2007-8-2-r19.
Huhn, A.S., Finan, P.H., 2021. Sleep disturbance as a therapeutic target to improve opioid use disorder treatment. Exp. Clin. Psychopharmacol. https://doi.org/10.1037/pha0000477. Advance online publication).
Jamali, K.A., Tramu, G., 1999. Control of rat hypothalamic pro-opiomelanocortin neurons by a circadian clock that is entrained by the daily light-off signal. Neuroscience 93 (3), 1051–1061. https://doi.org/10.1016/S0306-4522(99)00208-0.
Kerdelhue, B., Karteszi, M., Pasqualini, C., Reinberg, A., Mezey, E., Palkovits, M., 1983. Circadian variations in β-endorphin concentrations in pituitary and in some brain nuclei of the adult male rat. Brain Res. 261 (2), 243–248. https://doi.org/10.1016/0006-8993(83)90627-3.
King, C., Masserano, J.M., Codd, E., Byrne, W.L., 1981. Effects of β-endorphin and morphine on the sleep-wakefulness behavior of cats. Sleep 4 (3), 259–262. https://doi.org/10.1093/sleep/4.3.259.
Kojima, S., Shingle, D.L., Green, C.B., 2011. Post-transcriptional control of circadian rhythms. J. Cell Sci. 124 (3), 311–320. https://doi.org/10.1242/jcs.065771.
Labrecque, G., Vanier, M.C., 1995. Biological rhythms in pain and in the effects of opioid analgesics. Pharmacol. Ther. 68 (1), 129–147. https://doi.org/10.1016/0163-7258(95)02003-9.
Lee, H.S., Nelms, J.L., Nguyen, M., Silver, R., Lehman, M.N., 2003. The eye is necessary for a circadian rhythm in the suprachiasmatic nucleus. Nat. Neurosci. 6 (2), 111–112. https://doi.org/10.1038/nn1006.
LeGates, T.A., Fernandez, D.C., Hattar, S., 2014. Light as a central modulator of circadian rhythms, sleep and affect. Nat. Rev. Neurosci. 15 (7), 443–454. https://doi.org/10.1038/nrn3743.
Livak, K.J., Schmittgen, T.D., 2001. Analysis of relative gene expression data using real-time quantitative PCR and the 2−ΔΔCT method. Methods 25 (4), 402–408. https://doi.org/10.1006/meth.2001.1262.
Locklear, C.E., 2020. Opioids Disrupt Sleep and Wakefulness in C57BL/6J Mice. Master's Thesis. University of Tennessee. https://trace.tennessee.edu/utk_gradthes/6266.
Lu, X.Y., Shieh, K.R., Kabbaj, M., Barsh, G.S., Akil, H., Watson, S.J., 2002. Diurnal rhythm of agouti-related protein and its relation to corticosterone and food intake. Endocrinology 143 (10), 3905–3915. https://doi.org/10.1210/en.2002-220150.
Lupi, D., Oster, H., Thompson, S., Foster, R.G., 2008. The acute light-induction of sleep is mediated by OPN4-based photoreception. Nat. Neurosci. 11 (9), 1068–1073. https://doi.org/10.1038/nn.2179.
Matthes, H.W.D., Maldonadot, R., Simonin, F., Valverdet, O., Slowet, S., 1996. Loss of morphine-induced analgesia, reward effect and withdrawal symptoms in mice lacking the μ-opioid-receptor gene. Nature 383, 819–823. https://doi.org/10.1038/383819a0.
McDowell, K.A., Shin, D., Roos, K.P., Chesselet, M.F., 2014. Sleep dysfunction and EEG alterations in mice overexpressing alpha-synuclein. J Park Dis 4 (3), 531–539. https://doi.org/10.3233/JPD-140374.
Medzihradsky, F., 1976. Stereospecific binding of etorphine in isolated neural cells and in retina determined by a sensitive microassay. Brain Res. 108 (1), 212–219. https://doi.org/10.1016/0006-8993(76)90180-3.
Myer, E.C., Morris, D.L., Brase, D.A., Dewey, W.L., Zimmerman, A.W., 1990. Naltrexone therapy of apnea in children with elevated cerebrospinal fluid β-endorphin. Ann. Neurol. 27 (1), 75–80. https://doi.org/10.1002/ana.410270112.
Ono, D., Honma, K ichi, Honma, S., 2015. Circadian and ultradian rhythms of clock gene expression in the suprachiasmatic nucleus of freely moving mice. Sci. Rep. 5 (1), 12310 https://doi.org/10.1038/srep12310.
Orozco-Solís, R., Matos, R.J.B., Lopes de Souza, S., et al., 2011. Perinatal nutrient restriction induces long-lasting alterations in the circadian expression pattern of genes regulating food intake and energy metabolism. Int. J. Obes. 35 (7), 990–1000. https://doi.org/10.1038/ijo.2010.223.
Pack, A.I., Galante, R.J., Maislin, G., et al., 2007. Novel method for high-throughput phenotyping of sleep in mice. Physiol. Genom. 28 (2), 232–238. https://doi.org/10.1152/physiolgenomics.00139.2006.
Pilozzi, A., Carro, C., Huang, X., 2021. Roles of β-endorphin in stress, behavior, neuroinflammation, and brain energy metabolism. Int. J. Mol. Sci. 22 (1), 338. https://doi.org/10.3390/ijms22010338.
Przewlocka, B., Mogilnicka, E., Lason, W., van Luijtelaar, E.L.J.M., Coenen, A.M.L., 1986. Deprivation of REM sleep in the rat and the opioid peptides β-endorphin and dynorphin. Neurosci. Lett. 70 (1), 138–142. https://doi.org/10.1016/0304-3940(86)90452-0.
Quattrochi, L.E., Stabio, M.E., Kim, I., et al., 2019. The M6 cell: a small-field bistratified photosensitive retinal ganglion cell. J. Comp. Neurol. 527 (1), 297–311. https://doi.org/10.1002/cne.24556.
Rasmussen, N.A., Farr, L.A., 2003. Effects of morphine and time of day on pain and β-endorphin. Biol. Res. Nurs. 5 (2), 105–116. https://doi.org/10.1177/1099800403257166.
Raynor, K., Kong, H., Chen, Y., et al., 1993. Pharmacological characterization of the cloned K-, d-, mu-opioid receptors. Mol. Pharmacol. 45, 330–334. https://doi.org/10.1002/047120918X.emb0452.
Reddy, A.B., Karp, N.A., Maywood, E.S., et al., 2006. Circadian orchestration of the hepatic proteome. Curr. Biol. 16 (11), 1107–1115. https://doi.org/10.1016/j.cub.2006.04.026.
Richter, C., Woods, I.G., Schier, A.F., 2014. Neuropeptidergic control of sleep and wakefulness. Annu. Rev. Neurosci. 37 (1), 503–531. https://doi.org/10.1146/annurev-neuro-062111-150447.

Riou, F., Cespuglio, R., Jouvet, M., 1982. Endogenous peptides and sleep in the rat: II peptides without significant effect on the sleep-waning cycle. Neuropeptides 2 (5), 255–264. https://doi.org/10.1016/0143-4179(82)90015-4.
Rupp, A.C., Ren, M., Altimus, C.M., et al., 2019. Distinct ipRGC subpopulations mediate light's acute and circadian effects on body temperature and sleep. *eLife*. Published online 1–16. https://doi.org/10.7554/eLife.44358.001.
Russo, A.F., 2017. Overview of neuropeptides: awakening the senses? Headache 57 (Suppl. 2), 37–46. https://doi.org/10.1111/head.13084.
Saper, C.B., Chou, T.C., Scammell, T.E., 2001. The sleep switch: hypothalamic control of sleep and wakefulness. Trends Neurosci. 24 (12), 726–731. https://doi.org/10.1016/S0166-2236(00)02002-6.
Sawant, O.B., Horton, A.M., Zucaro, O.F., et al., 2017. The circadian clock gene Bmal1 controls thyroid hormone-mediated spectral identity and cone photoreceptor function. Cell Rep. 21 (3), 692–706. https://doi.org/10.1016/j.celrep.2017.09.069.
Scammell, T.E., Arrigoni, E., Lipton, J.O., 2017. Neural circuitry of wakefulness and sleep. Neuron 93 (4), 747–765. https://doi.org/10.1016/j.neuron.2017.01.014.
Schindelin, J., Arganda-Carreras, I., Frise, E., et al., 2012. Fiji: an open-source platform for biological-image analysis. Nat. Methods 9 (7), 676–682. https://doi.org/10.1038/nmeth.2019.
Schmidt, T.M., Chen, S.K., Hattar, S., 2011. Intrinsically photosensitive retinal ganglion cells: many subtypes, diverse functions. Trends Neurosci. 34 (11), 572–580. https://doi.org/10.1016/j.tins.2011.07.001.
Severino, A.L., Mittal, N., Hakimian, J.K., et al., 2020. μ-Opioid receptors on distinct neuronal populations mediate different aspects of opioid reward-related behaviors. eNeuro 7 (5), 2020. https://doi.org/10.1523/ENEURO.0146-20.2020. ENEURO.0146-20.
Sherin, J.E., Shiromani, P.J., McCarley, R.W., Saper, C.B., 1996. Activation of ventrolateral preoptic neurons during sleep. Science 271 (5246), 216–219.
Slaughter, M.M., Mattler, J.A., Gottlieb, D.I., 1985. Opiate binding sites in the chick, rabbit and goldfish retina. Brain Res. 339 (1), 39–47. https://doi.org/10.1016/0006-8993(85)90619-5.
Stütz, A.M., Staszkiewicz, J., Ptitsyn, A., Argyropoulos, G., 2007. Circadian expression of genes regulating food intake. Obesity 15 (3), 607–615. https://doi.org/10.1038/oby.2007.564.
Steiner, R.A., Kabigting, E., Lent, K., Clifton, D.K., 1994. Diurnal rhythm in proopiomelanocortin mRNA in the arcuate nucleus of the male rat. J. Neuroendocrinol. 6 (6), 603–608. https://doi.org/10.1111/j.1365-2826.1994.tb00625.x.
Tripathi, R., Rao, R., Dhawan, A., Jain, R., Sinha, S., 2020. Opioids and sleep – a review of literature. Sleep Med. 67, 269–275. https://doi.org/10.1016/j.sleep.2019.06.012.
Vandesompele, J., De Preter, K., Pattyn, F., et al., 2002. Accurate normalization of real-time quantitative RT-PCR data by geometric averaging of multiple internal control genes. Genome Biol. 3 (7) https://doi.org/10.1186/gb-2002-3-7-research0034 research0034.1-0034.11.
van der Veen, D.R., Gerkema, M.P., 2017. Unmasking ultradian rhythms in gene expression. Faseb. J. 31 (2), 743–750. https://doi.org/10.1096/fj.201600872R.
Voigt, T., 1986. Cholinergic amacrine cells in the rat retina. J. Comp. Neurol. 248 (1), 19–35. https://doi.org/10.1002/cne.902480103.
Wamsley, J.K., Palacios, J.M., Kuhar, M.J., 1981. Autoradiographic localization of opioid receptors in the mammalian retina. Neurosci. Lett. 27 (1), 19–24. https://doi.org/10.1016/0304-3940(81)90199-3.
Wang, Q., Yue, X.F., Qu, W.M., et al., 2013. Morphine inhibits sleep-promoting neurons in the ventrolateral preoptic area via mu receptors and induces wakefulness in rats. Neuropsychopharmacology 38 (5), 791–801. https://doi.org/10.1038/npp.2012.244.
Weibel, R., Reiss, D., Karchewski, L., et al., 2013. Mu opioid receptors on primary afferent Nav1.8 neurons contribute to opiate-induced analgesia: insight from conditional knockout mice. PLoS One 8 (9), e74706. https://doi.org/10.1371/journal.pone.0074706.
Whitney, I.E., Keeley, P.W., Raven, M.A., Reese, B.E., 2008. Spatial patterning of cholinergic amacrine cells in the mouse retina. J. Comp. Neurol. 508 (1), 1–12. https://doi.org/10.1002/cne.21630.
Wyman, J., Bultman, S., 2004. Postmortem distribution of heroin metabolites in femoral blood, liver, cerebrospinal fluid, and vitreous humor. J. Anal. Toxicol. 28 (4), 260–263. https://doi.org/10.1093/jat/28.4.260.
Xu, B., Kalra, P.S., Farmerie, W.G., Kalra, S.P., 1999. Daily changes in hypothalamic gene expression of neuropeptide Y, galanin, proopiomelanocortin, and adipocyte leptin gene expression and secretion: effects of food restriction. Endocrinology 140 (6), 2868–2875. https://doi.org/10.1210/endo.140.6.6789.
Zgierska, A., Brown, R.T., Zuelsdorff, M., Brown, D., Zhang, Z., Fleming, M.F., 2007. Sleep and daytime sleepiness problems among patients with chronic noncancerous pain receiving long-term opioid therapy: a cross-sectional study. J Opioid Manag 3 (6), 317–327. https://doi.org/10.5055/jom.2007.0020.
Zhang, J., Yang, Z., Wu, S.M., 2005. Development of cholinergic amacrine cells is visual activity-dependent in the postnatal mouse retina. J. Comp. Neurol. 484 (3), 331–343. https://doi.org/10.1002/cne.20470.
Zhang, Z., Beier, C., Weil, T., Hattar, S., 2021. The retinal ipRGC-preoptic circuit mediates the acute effect of light on sleep. Nat. Commun. 12 (1), 5115. https://doi.org/10.1038/s41467-021-25378-w.
Zhao, X., Stafford, B.K., Godin, A.L., King, W.M., Wong, K.Y., 2014. Photoresponse diversity among the five types of intrinsically photosensitive retinal ganglion cells. J. Physiol. 592 (7), 1619–1636. https://doi.org/10.1113/jphysiol.2013.262782.